IEEE Photonics Journal
An IEEE Photonics Society Publication

Open Access

Method for Receiving Weak Microwave Photonics Signals Based on Electro-Optical Up-Conversion

Volume 12, Number 4, August 2020

Qunsong He
Zijing Zhang
Jiaheng Xie
Zhiqiang Shen
Yuan Zhao

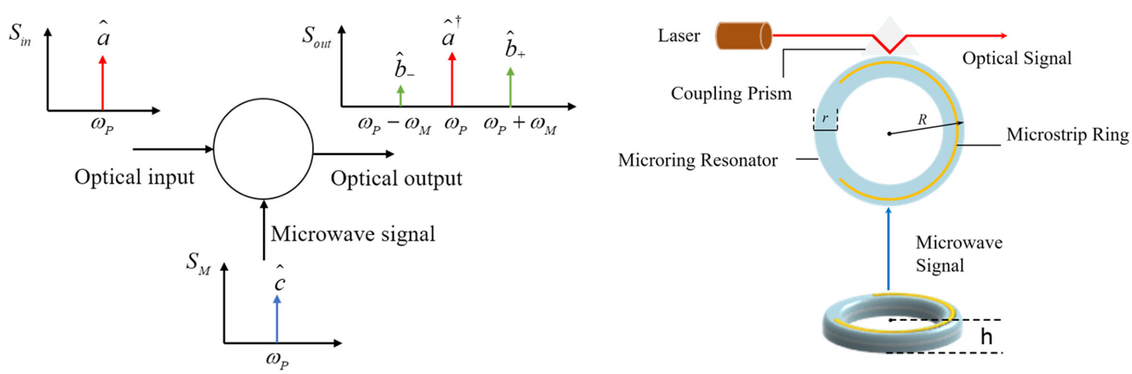

DOI: 10.1109/JPHOT.2020.3011427

IEEE photonics SOCIETY

IEEE

Method for Receiving Weak Microwave Photonics Signals Based on Electro-Optical Up-Conversion

Qunsong He, Zijing Zhang, Jiaheng Xie, Zhiqiang Shen, and Yuan Zhao

School of Physics, Harbin Institute of Technology, Harbin 150001, China

DOI:10.1109/JPHOT.2020.3011427

Manuscript received April 15, 2020; revised July 16, 2020; accepted July 20, 2020. Date of publication July 23, 2020; date of current version August 12, 2020. Corresponding author: Zhao Yuan (e-mail: zhaoyuan@hit.edu.cn).

Abstract: A novel method for receiving weak microwave photonics signals based on a micro-ring resonator is proposed. This approach uses the nonlinear interaction of a microwave and an optical pump to generate an up-conversion signal to achieve the signal reception. The minimum detectable power of this method reaches −89.79 dBm, which is suitable for the detection of weak signals. The power conversion efficiency and bandwidth have a 10 times promotion compared to similar conversion methods at room temperature. The result also demonstrates that the detection sensitivity can be improved by five orders of magnitude compared to the traditional modulators, and the output signal-to-noise ratio can be improved by more than 17 dB using a micro-ring resonator.

Index Terms: Microwave Photonics, micro-ring resonator, microwave receiver, microwave modulator.

1. Introduction

Microwave photonics processing has attracted much attention in recent years. Loading of microwave signals into fiber optic links has always been an important research topic [1]. However, the sensitivity of conventional electro-optic modulators has not been able to meet the requirements for a microwave photonics receiver (MPR).

The detection sensitivity of traditional modulators is limited, especially in a microwave photonics radar system. The echo signal received by radar antenna requires a series of adaptive amplification and filtering to meet the sensitivity requirements of existing electro-optic modulators. Current MPRs utilize Mach-Zehnder Interferometers (MZIs), with a sinusoidal transfer function as the electro-optical modulator, which results in a high driving power and a large receiver size. The modulators with low power, low drive voltage have been explored [2]–[5]. The driving voltage of the traditional modulator is at several volts [6], which brings high power consumption and other problems that cannot meet the needs of weak radar signal processing, which is a challenge for microwave photonics signal processing [7].

The efficient up-conversion of microwave signal to optical signal has become a popular research topic. Several studies based on cold atom, superconducting circuit [8], and high-quality mechanical films [9] have been conducted. Piezoelectric photonic crystals [10] have been used to connect electronic LC circuits and lasers to achieve up-conversion [11], [12]. However, the conversion

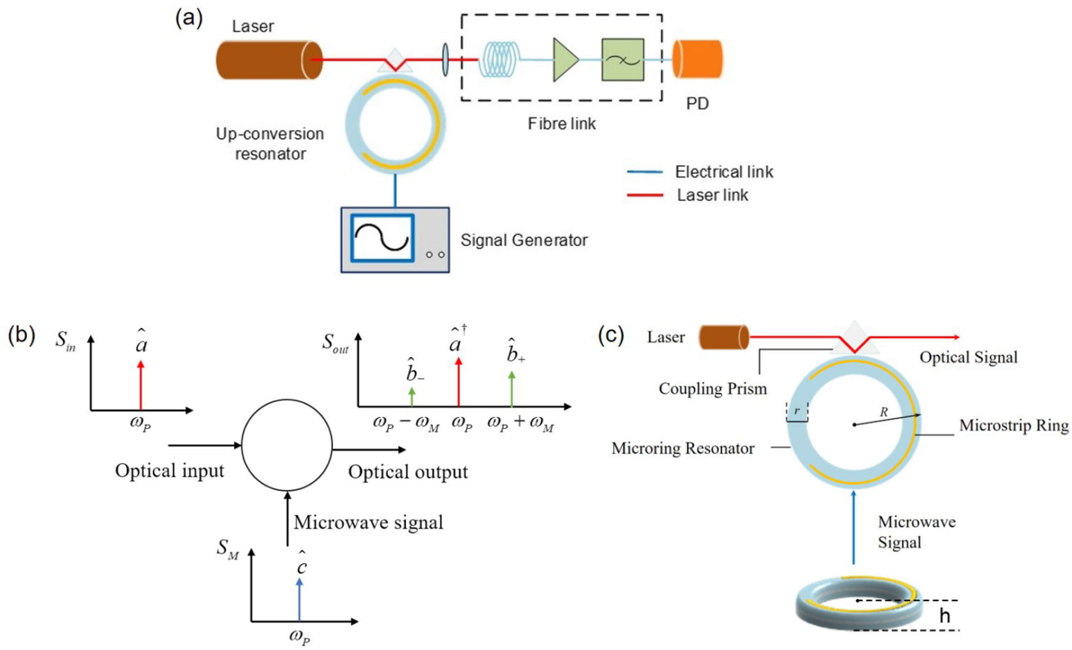

Fig. 1. (a) Schematic of the MPR using a micro-ring resonator. The red line is the laser beam, the blue line is the electronic circuit, and the light blue line is the optical fiber. (b) The spectra of the optical input signal S_{in}, the microwave signal S_M and the output optical signal S_{out} with multiple sidebands $\omega_P - \omega_M$ and $\omega_P + \omega_M$ generated by the modulator. (c) The micro-ring resonator for signals receiving with outer radius R, width r and thickness h.

efficiency of these methods is too low for room temperature applications. Whispering gallery mode (WGM) resonators have been introduced to realize the conversion of microwaves to an optical frequency and to achieve reception of weak microwave signal at room temperature [13]–[16]. The electro-optical conversion efficiency was improved by 3 orders of magnitude, and the power conversion efficiency reached 23.68 ± 0.46. But the conversion bandwidth of 1 MHz is limited in microwave photonics signal reception [17]. Compared with WGMs, the micro-ring resonator has similar photoelectric characteristics, which can provide higher conversion efficiency and solve the problem of bandwidth limitation in the receiving process.

We propose a novel microwave photonics signals receiving method for weak signal detection based on a high quality micro-ring resonator that supports the intensive nonlinear interaction between microwave and optical fields. The up-conversion efficiency of microwave signals to optical signals is improved through constraint of the overlapping region of the fields and the resultant enhancement of field interaction. Since no additional bias is required, the method has high detection sensitivity and signal-to-noise ratio (SNR), making it suitable for weak signals detection. The system described in this method can directly use the microwave signals received by the antenna and complete the process of electro-optic conversion and adaptive filtering. The system addresses the dilemma of high driving power of the electro-optic modulator and provides a method for the direct detection of weak microwave signals without complex post-processing.

2. Theoretical Analysis

A schematic of the weak microwave signals receiving setup is shown in Fig. 1(a). The optical pump from the distributed feedback laser feeds into the electro-optical up-conversion resonator by a coupling prism. In the resonator, the microwave signals and the optical carriers generate the up-conversion optical signals that contains the microwave information. The up-converted optical signals output from the coupling prism and feed into the optical fiber link to be received by the detector after amplification and filtering. The amplification and transmission of the up-conversion signals are analyzed to evaluate the weak microwave reception performance of the MPR.

The laser pump with angular frequency ω_P interacts with the microwave signals with angular frequency ω_M in the resonator, as shown in Fig. 1(b). The energy of the generated higher-order sidebands is extremely weak and only the generation of Stokes and anti-Stokes sidebands, with frequencies of $\omega_P - \omega_M$ and $\omega_P + \omega_M$, respectively, is considered. The adjacent cavity modes of the resonator are assumed to resonate with the frequency of the sidebands. The electric field intensity of the nonlinear process in the resonator can be expressed with the Hamiltonian $\hat{H}$ [18], [19]:

$$\hat{H} = \hbar g\left(\hat{a}\hat{b}_-^\dagger\hat{c}^\dagger + \hat{a}^\dagger\hat{b}_-\hat{c}\right) + \hbar g\left(\hat{a}\hat{b}_+^\dagger\hat{c} + \hat{a}^\dagger\hat{b}_+\hat{c}^\dagger\right) \tag{1}$$

Where $\hat{a}$, $\hat{a}^\dagger$, and $\hat{c}$, $\hat{c}^\dagger$, are the creation and annihilation operators of the optical pump and microwave signals, respectively. $\hat{b}_-$, $\hat{b}_-^\dagger$, and $\hat{b}_+$, $\hat{b}_+^\dagger$, are the generation and annihilation operators of the difference frequency and sum frequency signals, respectively. g denotes the strength of the nonlinear interaction in the resonator.

The mode of the electro-optical up-conversion was chosen to avoid unnecessary noise and interference due to the existence of weak and spontaneous optical down-conversion in the resonator [17]. The motion equations of particle interaction in the resonator, without considering the noise, are expressed as [19]

$$\frac{da}{dt} = -\gamma_P a - ig^*\left(b_- c + c^\dagger b_+\right) + E_P \tag{2}$$

$$\frac{db_-}{dt} = -\gamma_- b_- - igc^\dagger a \tag{3}$$

$$\frac{db_+}{dt} = -\gamma_+ b_+ - igca \tag{4}$$

$$\frac{dc}{dt} = -\gamma_M c - igb_-^\dagger a + ig^* a^\dagger b_+ + E_M \tag{5}$$

Where γ_P and γ_M are the optical and microwave decay coefficients, γ_+ and γ_- are the sum frequency and difference frequency decay coefficients, respectively. Assuming that the system is in a state of steady output, the values of Eqs. (2)–(5) will be zero. The electric field intensity of the sum frequency signals will then be

$$b_+ = \frac{-ig\gamma_M^*\gamma_- E_p E_M}{\gamma_+\gamma_-\gamma_P|\gamma_M|^2 + |g|\,|E_M|^2\left(\gamma_+ + \gamma_-\right)} \tag{6}$$

Where E_P and E_M are the intensity of the input electric field of the optical wave and microwave in the resonator, respectively.

The relationship between the power of the output optical signal and the input optical pump can be obtained by applying the transfer matrix method. Considering the nonlinear interaction in the cavity, the transfer matrix method is used to solve Eq. (6) and the relationship of the up-conversion optical power P_0, the input microwave power P_M, and the optical pump power P_P can be expressed as:

$$P_0 = \hbar Q_M\left(\frac{8gQ\omega_M\omega_P^2}{\hbar\omega_M^2\omega_P^3 + 32g^2 Q_M Q^2 P_M}\right)^2 P_P P_M \tag{7}$$

Where $Q = \omega_P/(2\gamma_P)$ and $Q_M = \omega_M/(2\gamma_M)$ are the quality factors of the optical and microwave resonators, respectively.

Considering that the input microwave power P_M as a small signal approximately, Eq. (7) can be simplified as $P_0 = \eta P_M$, where η is the power conversion efficiency in up-conversion and can be expressed as:

$$\eta = \left(\frac{8gQ}{\omega_P}\right)^2 \frac{Q_M}{\hbar\omega_M^2} P_P \tag{8}$$

The power will be modified by the optical fiber during transmission. A, ε and μ are the cross-sectional area, dielectric constant and permeability of the optical fiber respectively. The output optical power is modified to be

$$P_0 = \frac{A}{2}\left(\frac{\varepsilon}{\mu}\right)^{\frac{1}{2}} \left(\frac{8gQ}{\omega_P}\right)^2 \frac{Q_M}{\hbar\omega_M^2} P_P P_M \tag{9}$$

The photocurrent received by the photodetector is $I(t) = \gamma_0 P_M$, where γ_0 denotes the optical power conversion coefficientl. The output power of photodetector is $P_{\text{out}} = \gamma_0^2 R_0 P_M^2$, in which R_0 denotes the resistance of the photodetector and

$$\gamma_0 = \Re\frac{A}{2}\left(\frac{\varepsilon}{\mu}\right)^{\frac{1}{2}} \left(\frac{8gQ}{\omega_P}\right)^2 \frac{Q_M}{\hbar\omega_M^2} P_P \tag{10}$$

Where $\Re$ denotes the responsivity of photodetector.

3. Simulation and Analysis

A micro-ring resonator with high quality factor is used to construct the electro-optic up-conversion resonator. The electro-optic up-conversion resonator structure is shown in Fig. 1(c). The optical pump feeds into the left port and the up-converted optical signal outputs from the right port of the coupling prism. The input optical pump and microwave signal interact in the resonator. The resonator is based on a lithium niobate crystal and it can be placed in a three-dimensional metal box to constrain the electromagnetic field. The input optical field is fed into the resonator by prism coupling or fiber coupling. The outer radius and width of the micro-ring are R and r, respectively, and the thickness of the micro-ring resonator is h. A microstrip ring is laid on the surface of the lithium niobate crystal, and a microwave signal is transmitted to the microstrip ring through microstrip lines, which interact with the optical field inside the resonator cavity to achieve microwave reception. The structure is designed to match the optical and microwave modes in the lithium niobate crystal.

The strength of the interaction g in the electro-optic up-conversion resonator can be expressed as [17]

$$g = \omega_P \chi^{(2)} \frac{n_a n_b}{n_c} \sqrt{\frac{\pi\hbar\omega_M}{2V}} \left(\frac{1}{V}\int_V dV \Psi_a^* \Psi_b \Psi_c\right) \tag{11}$$

Where Ψ_a, Ψ_b, and Ψ_c are the normalized electric field distributions of optical pump, sum frequency signal and microwave signal in the optical cavity. n_a, n_b, and n_c are the effective refractive indices of the signals with the corresponding frequencies in the resonant cavity and $\chi^{(2)}$ is the second-order nonlinear strength of the nonlinear crystal. The normalized mode volume V is defined as the integral of the square of the absolute value of the eigenfunction and the interaction strength is related to the distribution of the microwave and optical fields.

The interaction strength between the microwave and optical fields determines the conversion efficiency. The optical field distribution is constrained in the edge region of the disk in WGM mode and the conversion efficiency is limited by the overlap of microwave and optical fields. Therefore, the optical field can be constrained within the cavity by controlling the radius and thickness of the micro-ring resonator. The energy density of microwave and optical wave are higher in the micro-ring resonator, which greatly increases the overlap factor and achieves higher conversion efficiency compared to the WGM. The resonance wavelength and free spectral range (FSR) of the micro-ring resonator can be determined by the structure of the micro-ring as:

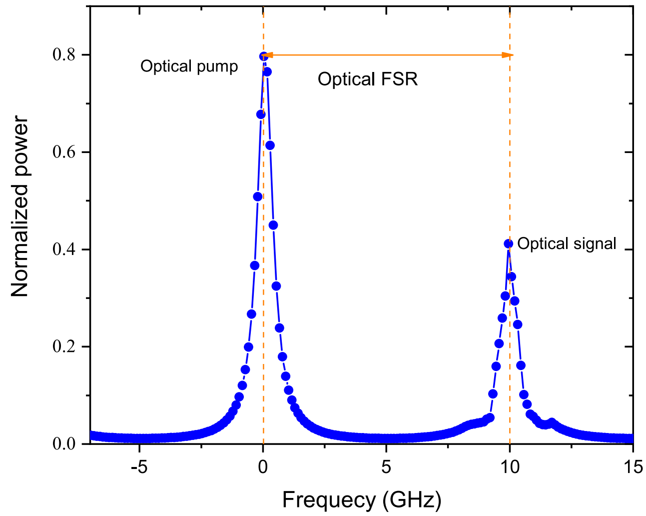

Fig. 2. Normalized power versus frequency with the optical pump and the up-conversion optical signal indicated by dotted lines.

$$2\pi Rn_g = m\lambda \tag{12}$$

$$FSR = \frac{c}{2\pi Rn_g} \tag{13}$$

Where R is the outer radius of the micro-ring, n_g is the effective refractive index of optical propagation in the cavity, c is the velocity of light in vacuum, λ is the wavelength of optical carrier in the cavity, and $m = 1, 2, 3, \ldots$ is the number of resonance stages.

$$P_0 = 8P_P P_M \left(\frac{\sqrt{\hbar\omega_M\omega_P}}{2g\sqrt{Q_M}Q} + \frac{2g\sqrt{Q_M}Q}{\sqrt{\hbar\omega_M\omega_P}} \cdot 8P_M \right)^{-2} \leq P_P/2 \tag{14}$$

From Eq.(7), the up-conversion signal power P_0 can be expressed as Eq.(14), due to the existence of down-conversion, the up-conversion signal power will less than the half of pump light power. The wavelength of the adopted input optical pump is 1550 nm and the microwave frequency is 10 GHz. As shown in Fig. 2, the system is in the steady state hypothetically. The up-converted optical signal meets the saturation state that limited by the interaction strength g, and the up-conversion optical signal power will be half of the pump light power.

In the band of 1550 nm, the dispersion of lithium niobate is weak and the resonant mode of the optical cavity satisfies the isometric condition. The system operates in the critical coupling state, and the upconversion signal 3-dB bandwidth is 19.34 MHz.The microwave frequency needs satisfy $\omega_M = FSR$ to achieve the highest conversion efficiency. In lithium niobate crystals [20], the refractive indexes of optical pump and sum frequency signals are $n_a = 2.21$, $n_b = 2.21$, we ignore the dispersion since the up-conversion signal is close to the pump light signal frequency [21]. The resonator radius is then calculated to be $R = 2.39$ mm, according to Eqs. (12)-(13).

With the determined resonant cavity material and signal frequency, g is mainly affected by the normalized mode volume V, the interaction inside the cavity is changed with V. COMSOL commercial software is used to simulate the electric field distribution of the micro-ring resonator. Anisotropic medium tensor material model is used in the simulation of lithium niobate [22], [23].

The width of the microstrip ring is $w = 0.1$ μm as shown in Fig. 3(a). The cavity operates in a critical coupling state and the resonant frequency is $\omega_M = m_M c/\alpha R n_M$, where α is the microstrip angular length, n_M the effective refractive index in the microwave range whose value is affected by the material and size [23]. The phase matching condition requires that $n_g(\omega_0 - \omega_c) = n_M\omega_M$. The

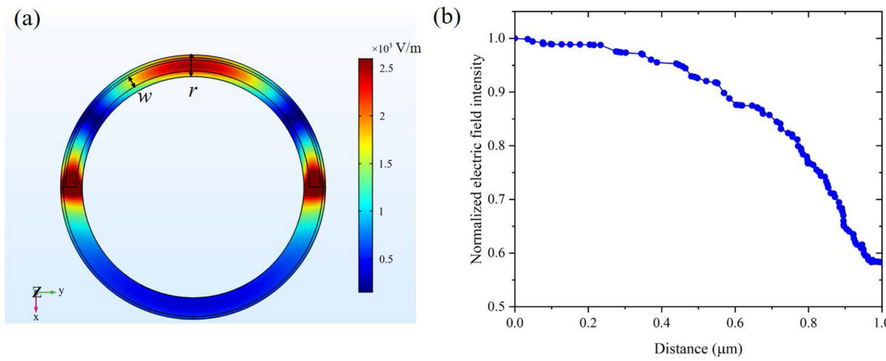

Fig. 3. (a) The distribution of microwave electric field in the cavity with $\alpha = \pi$ and the microwave modes $m_M = 1$. The vertical to the inside is in the z-axis. (b) The distribution of microwave field intensity along the z-axis in the cavity, the zero point is located at the interface between the resonator and the microstrip ring.

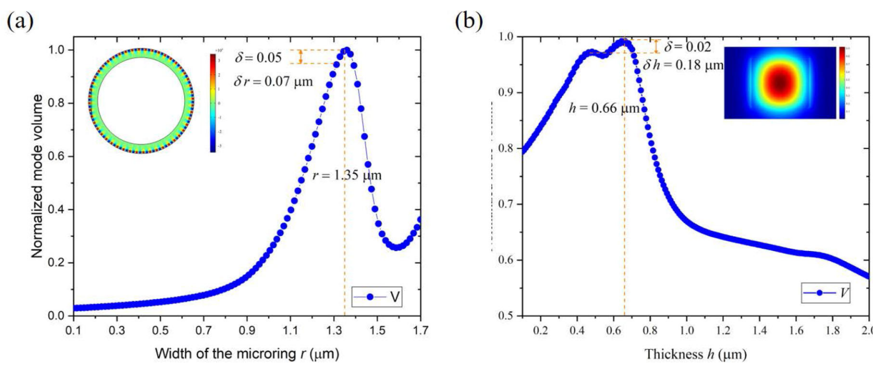

Fig. 4. (a) The curve of normalized mode volume V versus width of the micro-ring resonator, the inset is the electric field distribution of the circular section of the micro-ring resonator. (b) The curve of normalized mode volume V versus the thickness of the micro-ring resonator, the inset is the electric field distribution of the cross section of the micro-ring resonator.

effective refractive index for a single mode can be geometrically engineered, such as the proportion of electric field energy in the air. Turning the thickness of dielectric is an effective way to engineer n_M. The tolerances are discussed below. The distribution of microwave electric field in the cavity with $\omega_M = 10$ GHz is shown in Fig. 3(a), where $\alpha = \pi$ and the number of microwave modes m_M is 1. The distribution of microwave field intensity along the z-axis is shown in Fig. 3(b). The intensity of microwave electric field gradually decreases with the increase of thickness of the dielectric cavity. A thicker dielectric cavity will weaken the constraint of the optical field and reduce the coupling intensity of the microwave field and the optical field.

The overlap of the optical and microwave fields in the resonator is also affected by the width of the micro-ring resonator r as shown in Fig. 1(c). The optical field inside the resonator cavity is constrained laterally in the direction of the parallel resonator cavity. A larger r will generate a higher order mode in the resonator, that reducing the normalized mode volume V. A small r will lead to mode leakage, resulting in a sharp reduction in V. The interaction of the microwave field in the overlapping area will reach the maximum at $r = 1.35\ \mu$m, the normalized mode volume V will be the largest, with an acceptable tolerance δr about 0.07 μm, and the change in V is less than $\delta =$ 5%, as shown in Fig. 4(a). Similarly, the overlap integral of the field affected by the thickness of the resonator cavity is shown in Fig. 4(b). The optical field inside the resonator is constrained in

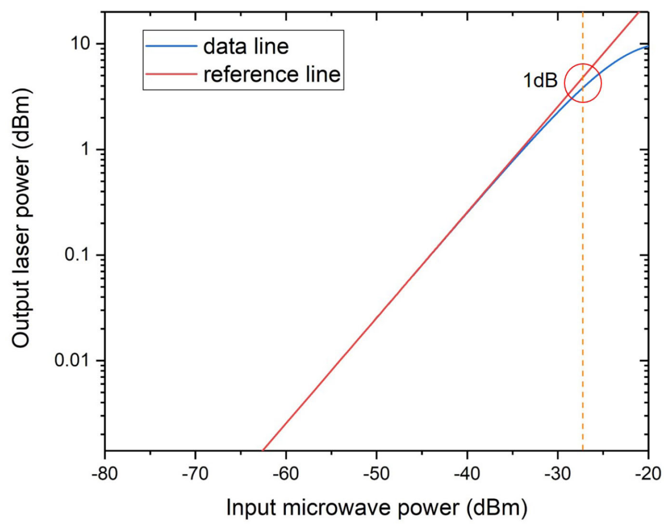

Fig. 5. Plot of output laser power versus input microwave power. The blue curve represents the relationship between the simulated input microwave power and the up-conversion optical signal power. The red curve is a linear reference line.

the direction of the vertical resonator. The interaction between the optical field and the microwave field in the overlapped area decreases with decreasing thickness h. The optical field will not be confined inside the crystal as the thickness decreases, which results in a gradually weakening interaction between the optical field and the microwave field. When the thickness $h = 0.66$ μm, the normalized mode volume V reaches its largest value. At $h = 0.66$ μm, a tolerance δh about 0.18 μm is acceptable, and the change in V is less than $\delta = 2\%$.

It is worth pointing out that fabrication does not need to achieve accurate phase compensation, because the phase matching can be fine-tuned by changing the microwave dispersion of the system. The conceivable fabrication error is tolerable and solvable by a flexible aluminium drumhead embedded in a microwave circuit. An adjustment of microwave frequency above 0.5 GHz without significantly reducing the quality factor has been achieved [24].

4. Detection Sensitivity and SNR

The up-conversion efficiency in the resonator can be calculated by using the simulation results. Since recent publications demonstrate a nearly critically coupled lithium niobate microring resonator with an intrinsic $Q \approx 10^7$ [25], and the increasing of the waveguide width leads to a Q improvement, we assume that the quality factors are $Q = 10^7$ and $Q_M = 100$ in the calculation. As $Q = \omega/\delta\omega$, with ω to be the optical resonance frequency and $\delta\omega$ to be the optical bandwidth, the optical bandwidth should be 19.34 MHz.

From simulations above, Eq. (11) is calculated to prove the interaction strength $g = 494.39$ in the electro-optic up-conversion resonator, which is about 10 times compared to a traditional microdisk resonator [17]. According to Eq. (7), this g value results in a significant improvement of the conversion efficiency and enhances the output up-conversion optical power P_0. It can be obtained from Eq. (8) that power conversion efficiency is $\eta = 2.54 \times 10^2$ with pump power $P_P = 1$ mW. The detection sensitivity and SNR of the MPR is related to the up-conversion optical power.

The relationship between the up-conversion optical power and the input microwave power is shown in Fig. 5. The blue curve in Fig. 5 represents the relationship between the input microwave power and the optical signal power. The red line in Fig. 5 is a linear reference line. The output power of the optical signal is a function varying with P_M in Eq. (7). With the gradual increase of P_M to $\hbar\omega_M^2\omega_P^2/32g^2Q_MQ^2$, the up-converted signal becomes saturated. The power conversion efficiency is

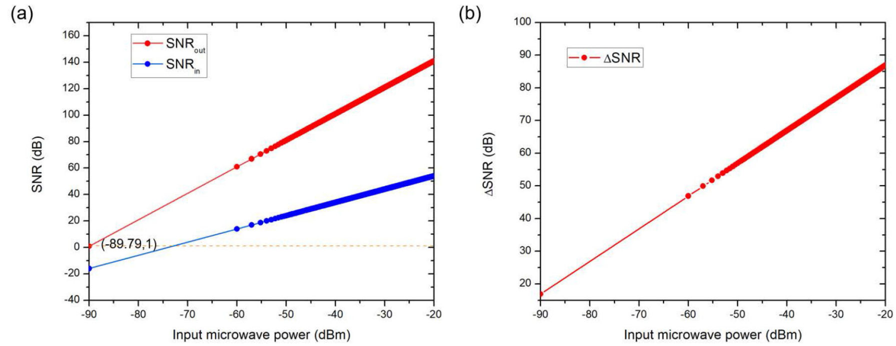

Fig. 6. (a) SNR versus input microwave power wherein the red and blue lines indicate the output and input SNR, respectively, of the MPR. (b) ΔSNR versus input microwave power wherein the red line indicates the difference between the input and output SNR.

limited by the quality factor of resonator. The output optical signal is compressed by 1 dB relative to the linear response of the system at $P_M = -27.25$ dBm. A large dynamic range of 62.54 dB signal reception is achieved below an input power of $P_M = -27.25$ dBm in this weak MPR scheme.

Next, the microwave thermal noise within the microwave signal, the shot noise, and the relative intensity noise in the fiber and detector, are considered [26]. The input SNR is $SNR_{\text{in}} = P_M/KTG(f)$, where $G(f)$ is the filter function of the electro-optical up-conversion cavity. We assume the bandwidth is 19.34 MHz. After electro-optical up-conversion and optical link transmission, shot noise N_s, and relative intensity noise N_{RIN} of pump light are introduced, which affect the output SNR of the setup. The corresponding noise can be expressed as,

$$N_s = 2q\gamma_0 P_M R_0 G(f) \tag{15}$$

$$N_{RIN} = \frac{1}{2} 10^{\frac{RIN}{10}} (\gamma_0 P_M)^2 R_0 G(f) \tag{16}$$

Where K is Boltzmann constant, T is the environment temperature, and R_0 is the resistance of photodetector. RIN is the relative intensity noise of the pump light. The output signal can be obtained by Eq.(9), and the output SNR can be expressed as,

$$SNR_{\text{out}} = \frac{\gamma_0^2 R_0 P_M^2}{2q\gamma_0 P_M R_0 G(f) + \frac{1}{2} 10^{\frac{RIN}{10}} (\gamma_0 P_M)^2 R_0 G(f) + \gamma_0 KTG(f)} \tag{17}$$

The setup is at room temperature environment with T being 300 K. The photodetector has a responsivity of 0.75 A/W and a resistance of $R_0 = 50\ \Omega$. The typical value of relative intensity noise of laser is $RIN = -155$ dBm/Hz [27].

The relationship between the output SNR and the input SNR of the system is found by solving Eq. (9) and is shown in Fig. 6. It can be seen that the output SNR of the MPR is improved by more than 17 dB compared to the input SNR. This improvement increases with the increase of the input power. When the input microwave power is -27.25 dBm, the increment ΔSNR of the output signal will be 79 dB.

In the receiver setup, the detection sensitivity S of the microwave signal is related to the SNR and is given by

$$S = \frac{2q\gamma_0 P_M R_0 + \frac{1}{2} 10^{\frac{RIN}{10}} (\gamma_0 P_M)^2 R_0 + \gamma_0 KT}{\gamma_0^2 R_0} \tag{18}$$

When the output SNR reaches the minimum detectable value where $SNR_{\text{out}} = 1$, as shown in Fig. 6(a), the minimum detectable power is -89.79 dBm (1.05×10^{-9} mW). This result shows large improvement in detection sensitivity of the microwave photonics receiver compared to a traditional electro-optic modulator where the minimum driving power is about 1×10^{-4} mW. With the micro-ring method, the detection sensitivity has been improved by five orders of magnitude [28], [29]. The power conversion efficiency is around $\eta = 2.54 \times 10^2$ and the bandwidth is 19.34 MHz, which are 10 times better compared to state-of-art power conversion efficiency [17]. It is worth noting that amplification and filtering of the optical fiber link will further improve the output SNR of the system, the sensitivity can be improved by increasing the gain under the background of the weak microwave signal.

5. Conclusion

A new setup for weak microwave signal reception, which is suitable for processing weak microwave signals under strong background noise, is proposed. The MPR detection sensitivity has been significantly increased in comparison to the traditional microwave photonics receiver method. A microwave driving power of one microwatt, which is required by the traditional electro-optic modulator, is reduced to a picowatt by the proposed method; a five orders of magnitude increase in detection sensitivity is achieved. The power conversion efficiency is 10 times higher compared to state-of-art microwave receivers. The proposed method significantly improves the detection sensitivity and SNR of the microwave photonics receiver and provides the possibility of direct detection of weak microwave signals while meeting the requirements for device integration.

References

[1] C. Wang *et al.*, "Integrated lithium niobate electro-optic modulators operating at cmos-compatible voltages," *Nature*, vol. 562, no. 7725, pp. 101–104, 2018.

[2] V. Sorianello *et al.*, "Graphene–silicon phase modulators with gigahertz bandwidth," *Nature Photon.*, vol. 12, no. 1, pp. 40–44, 2018.

[3] M. G. Wood *et al.*, "Gigahertz speed operation of epsilon-near-zero silicon photonic modulators," *Optica*, vol. 5, no. 3, pp. 233–236, 2018.

[4] F. Sun *et al.*, "The all-optical modulator in dielectric-loaded waveguide with graphene-silicon heterojunction structure," *Nanotechnology*, vol. 29, no. 13, 2018, Art. , no. 135201.

[5] B. Dingel, N. Madamopoulos, A. Prescod, and R. Madabhushi, "Analytical model, analysis and parameter optimization of a super linear electro-optic modulator (SFDR > 130 db)," *Opt. Commun.*, vol. 284 , no. 24, pp. 5578–5587, 2011.

[6] C. Wang *et al.*, "Integrated lithium niobate electro-optic modulators operating at CMOS-compatible voltages," *Nature*, vol. 562, no. 7725, pp. 101–104, 2018.

[7] D. Marpaung, J. Yao, and J. Capmany, "Integrated microwave photonics," *Nature Photon.*, vol. 13, no. 2, pp. 80–90, 2019.

[8] C. Javerzac-Galy, K. Plekhanov, N. Bernier, L. D. Toth, A. K. Feofanov, and T. J. Kippenberg, "On-chip microwave-to-optical quantum coherent converter based on a superconducting resonator coupled to an electro-optic microresonator," *Phys. Rev. A*, vol. 94, no. 5, 2016, Art. , no. 053815.

[9] R. W. Andrews *et al.*, "Bidirectional and efficient conversion between microwave and optical light," *Nature Phys.*, vol. 10, no. 4, pp. 321–326, 2014.

[10] M. Goryachev, N. Kostylev, and M. E. Tobar, "Single-photon level study of microwave properties of lithium niobate at millikelvin temperatures," *Phys. Rev. B*, vol. 92, no. 6, 2015, Art. no. 060406.

[11] J. Bochmann, A. Vainsencher, D. D. Awschalom, and A. N. Cleland, "Nanomechanical coupling between microwave and optical photons," *Nature Phys.*, vol. 9, no. 11, pp. 712–716, 2013.

[12] T. Wang, T. Wang, C. Fu, and X. Su, "Using reservoir-engineering to convert a coherent signal in optomechanics with small optomechanical cooperativity," *Phys. Lett. A*, vol. 381, no. 18, pp. 1629–1633, 2017.

[13] Y. Ehrlichman, A. Khilo, and M. A. Popović, "Optimal design of a microring cavity optical modulator for efficient rf-to-optical conversion," *Opt. Exp.*, vol. 26, no. 3, pp. 2462–2477, 2018.

[14] D. Cohen, M. Hossein-Zadeh, and A. Levi, "High-Q microphotonic electro-optic modulator," *Solid-State Electron.*, vol. 45, no. 9, pp. 1577–1589, 2001.

[15] N. Pavlov, N. Kondratyev, and M. Gorodetsky, "Modeling the whispering gallery microresonator-based optical modulator," *Appl. Opt.*, vol. 54, no. 35, pp. 10 460–10 466, 2015.

[16] I. Lekavicius, D. A. Golter, T. Oo, and H. Wang, "Transfer of phase information between microwave and optical fields via an electron spin," *Phys. Rev. Lett.*, vol. 119, no. 6, 2017, Art. no. 063601.

[17] A. Rueda *et al.*, "Efficient microwave to optical photon conversion: An electro-optical realization," *Optica*, vol. 3, no. 6, pp. 597–604, 2016.

[18] G. S. Botello *et al.*, "Sensitivity limits of millimeter-wave photonic radiometers based on efficient electro-optic upconverters," *Optica*, vol. 5, no. 10, pp. 1210–1219, 2018.

[19] M. Tsang, "Cavity quantum electro-optics. II. input-output relations between traveling optical and microwave fields," *Phys. Rev. A*, vol. 84, no. 4, 2011, Art. no. 043845.

[20] R. Hosseini, L. Mirzoyan, and K. Jamshidi, “Energy consumption enhancement of reverse-biased silicon-based Mach–Zehnder modulators using corrugated slow light waveguides,” *IEEE Photon. J.*, vol. 10, no. 1, Feb. 2018, Art. no. 8200207.
[21] G. Edwards and M. Lawrence, “A temperature-dependent dispersion equation for congruently grown lithium niobate,” *Opt. Quantum Electron.*, vol. 16, no. 4, pp. 373–375, 1984.
[22] L. Cai *et al.*, “Acousto-optical modulation of thin film lithium niobate waveguide devices,” *Photon. Res.*, vol. 7, no. 9, pp. 1003–1013, 2019.
[23] N. Pavlov, N. Kondratyev, and M. Gorodetsky, “Modeling the whispering gallery microresonator-based optical modulator,” *Appl. Opt.*, vol. 54, no. 35, pp. 10 460–10 466, 2015.
[24] R. Andrews, A. Reed, K. Cicak, J. Teufel, and K. Lehnert, “Quantum-enabled temporal and spectral mode conversion of microwave signals,” *Nature Commun.*, vol. 6, 2015, Art. no. 10021.
[25] M. Zhang, C. Wang, R. Cheng, A. Shams-Ansari, and M. Lončar, “Monolithic ultra-high-Q lithium niobate microring resonator,” *Optica*, vol. 4, no. 12, pp. 1536–1537, 2017.
[26] A. Ramaswamy *et al.*, “Integrated coherent receivers for high-linearity microwave photonic links,” *J. Lightw. Technol.*, vol. 26, no. 1, pp. 209–216, 2008.
[27] C. W. Nelson, A. Hati, and D. A. Howe, “Relative intensity noise suppression for RF photonic links,” *IEEE Photon. Technol. Lett.*, vol. 20, no. 18, pp. 1542–1544, Sep. 2008.
[28] B. Baeuerle *et al.*, “120 gbd plasmonic Mach-Zehnder modulator with a novel differential electrode design operated at a peak-to-peak drive voltage of 178 mv,” *Opt. Express*, vol. 27, no. 12, pp. 16 823–16 832, 2019.
[29] M. Moralis-Pegios *et al.*, “52 km-long transmission link using a 50 gb/s O-band silicon microring modulator co-packaged with a 1V-CMOS driver,” *IEEE Photon. J.*, vol. 11, no. 4, Aug. 2019, Art. no. 7903907.